

### Electronic Supplementary Information

**Table S1.** Comparison of different fluorescence probes for GSH detection based on MnO<sub>2</sub> nanosheets.

Probes	stokes shift (nm)	LOD (nM)	Assay time (min)	Refs
Scopoletin & Amplex Red	85 and 25	6.7	Not given	10
Boron nitride quantum dots	70	160	6	11
Carbon dots	75	300	3	23
Carbon quantum dots	97	300	5	24
Graphene quantum dot	90	150	6	25
Semiconductor quantum dots	170	10	10	26
BSA-Cu NCs	75	100	5	27
g-C <sub>3</sub> N <sub>4</sub> Nanosheet	78	200	6	28
AIE-silica nanospheres	120	200	5	29
Polymer dots	100	100	15	41
AIE-Cys-Cu NCs	235	1.2	3	This work

**Table S2.** Nanosecond time-resolved luminescence transients of Cu NCs in the absence and presence of MnO<sub>2</sub> nanosheets. The luminescence of Cu NCs (maximum wavelength,  $\lambda_{\text{max}}=593$  nm) was detected with a 375 nm excitation laser. Numbers in parentheses indicate relative weightage.

system	$\tau_1$ (ns)	$\tau_2$ (ns)	$\tau_{\text{av}}$ (ns)
Cu NCs	6.26 (0.72%)	0.16 (99.28%)	0.2036
Cu NCs + MnO <sub>2</sub>	6.36 (0.21%)	0.19 (99.79%)	0.2057

**Table S3.** Determination result of GSH in human serum samples.

Method	Sample 1	Sample 2	Sample 3	Sample 4	Sample 5
This method/ $\mu\text{M}$	2.43	2.41	2.15	2.83	1.97
OPA probe/ $\mu\text{M}$	2.38	2.27	2.09	2.78	2.06

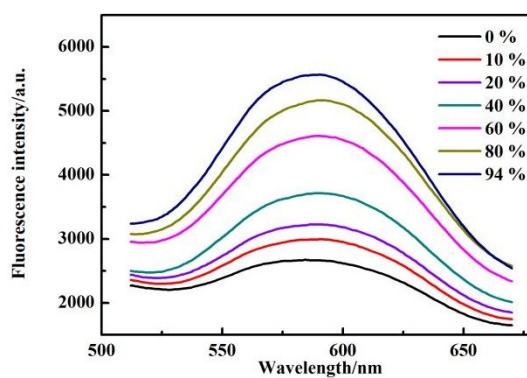


**Fig. S1.** The fluorescence spectra of the Cu NCs in mixed solvents of ethanol and water with different volumetric fractions of ethanol.

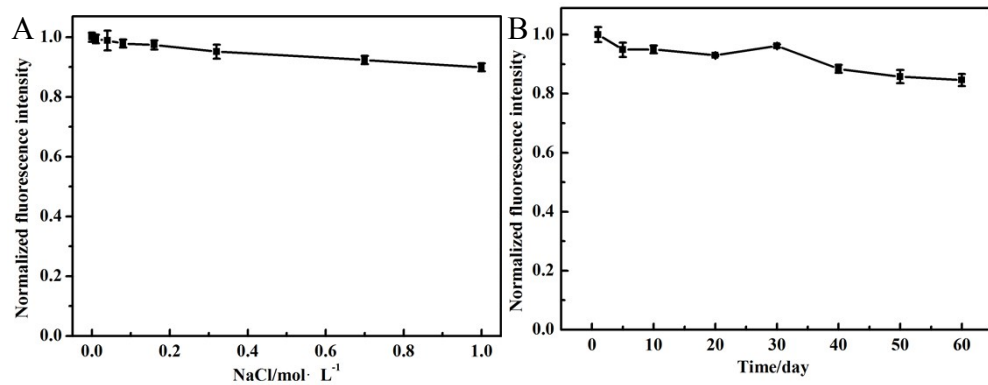


**Fig. S2.** (A) The effect of NaCl concentration on the FL response of Cu NCs. (B) The effect of storage time on FL response of Cu NCs.

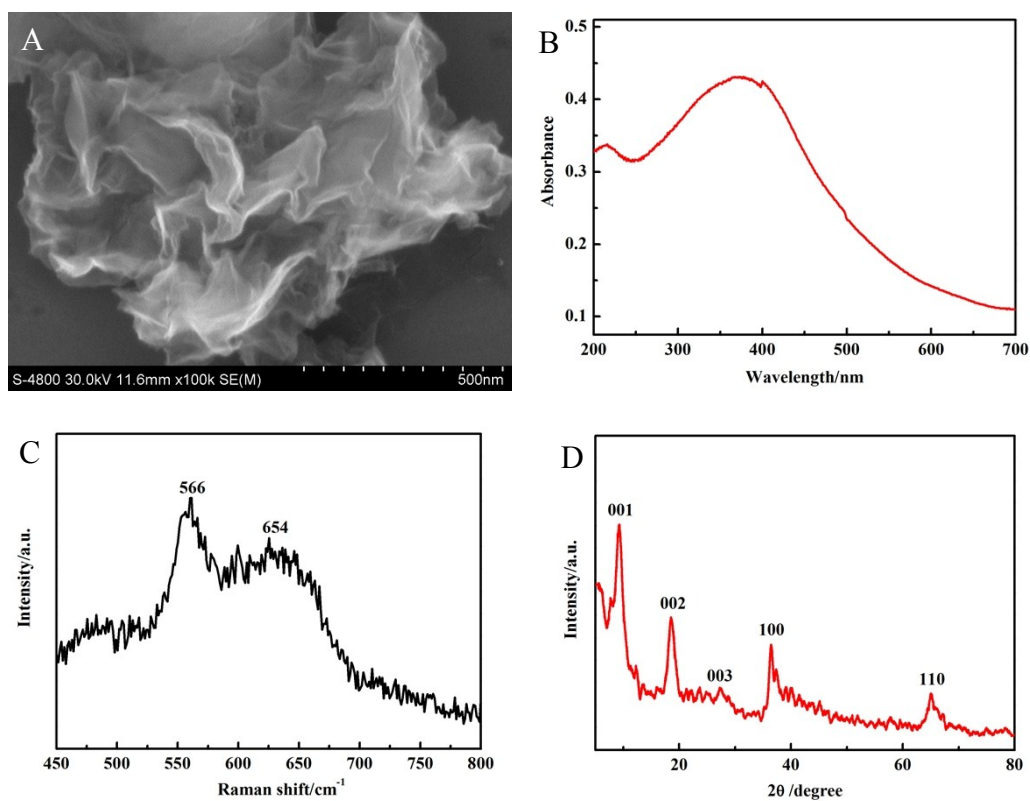


**Fig. S3.** The SEM image (A), the UV-Vis absorption spectra (B), Raman spectrum (C) and XRD spectra (D) of MnO<sub>2</sub> nanosheets.

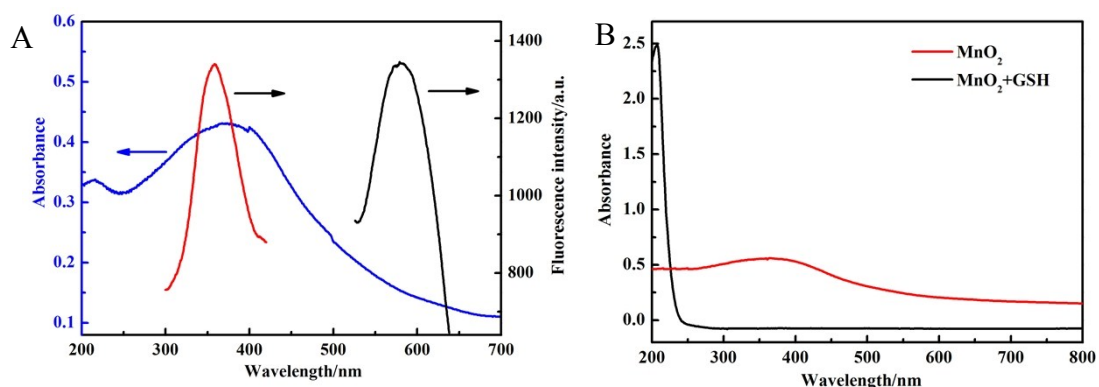


**Fig. S4.** (A) Fluorescence excitation (red curve) and emission (black curve) spectra of Cu NCs, and UV-vis absorption spectrum of MnO<sub>2</sub> nanosheets (blue curve). (B) UV-vis absorption spectrum of MnO<sub>2</sub> nanosheets in the absence (red line) and presence of GSH (black line).

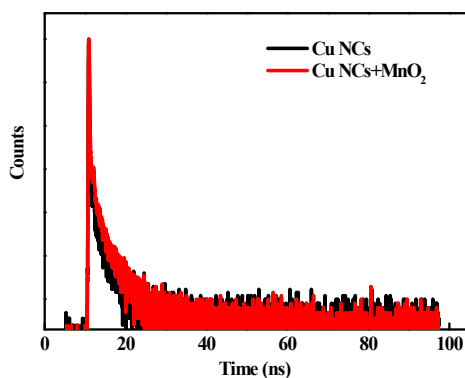


**Fig. S5.** Decay curves of Cu NCs in the absence and presence of MnO<sub>2</sub> nanosheets. The maximum excitation and emission wavelengths are 375 nm and 593 nm, respectively.

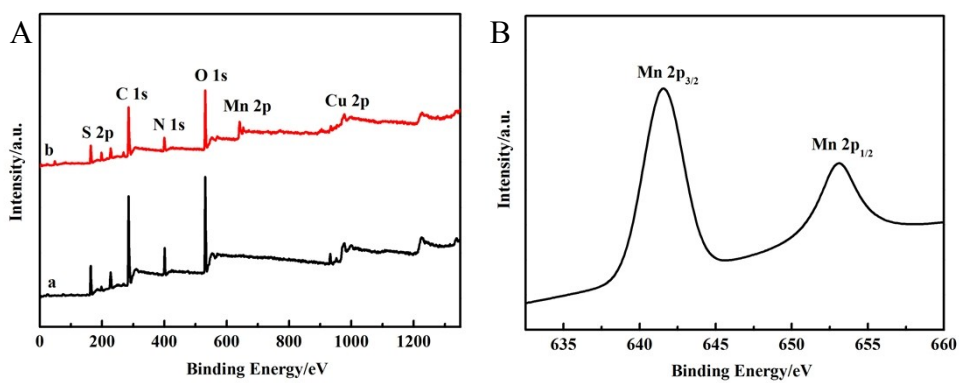


**Fig. S6.** (A) XPS spectra of Cu NCs in the absence (a) and presence of MnO<sub>2</sub> nanosheets (b). (B) XPS spectrum in the Mn 2p of Cu NCs-MnO<sub>2</sub> system.

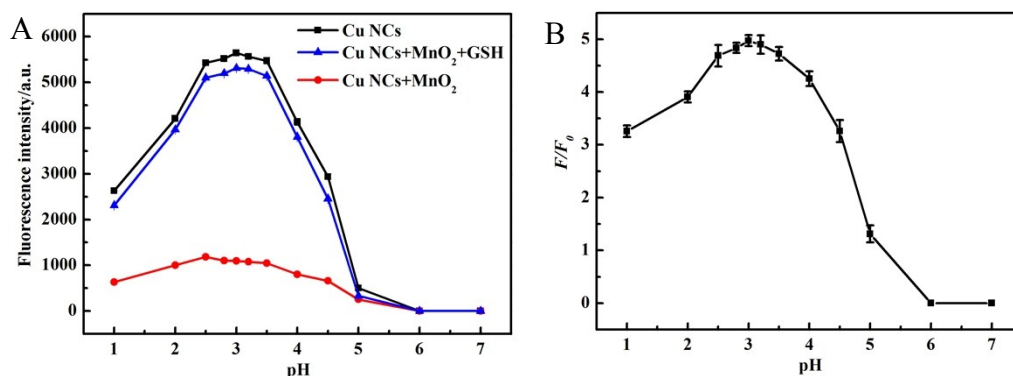


**Fig. S7.** (A) Effect of pH on the FL response of Cu NCs, Cu NCs-MnO<sub>2</sub> nanosheets and Cu NCs-MnO<sub>2</sub> nanosheets-GSH systems. (B) Effect of solution pH on  $F/F_0$  value. The concentrations of Cu NCs, MnO<sub>2</sub> nanosheets and GSH were 0.5 mM, 100  $\mu$ g/mL and 90  $\mu$ M, respectively. Error bars were the standard deviation of three independent experiments.

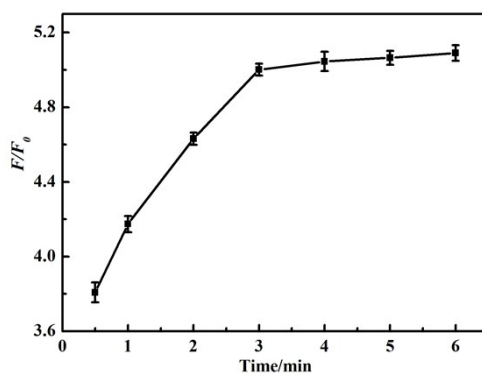


**Fig. S8.** Effect of reaction time on the fluorescence of Cu NCs-MnO<sub>2</sub> nanosheets system for detecting GSH. The concentrations of Cu NCs, MnO<sub>2</sub> nanosheets and GSH were 0.5 mM, 100  $\mu$ g/mL and 90  $\mu$ M, respectively. Error bars were the standard deviation of three independent experiments.